PHYSICAL REVIEW B
CONDENSED MATTER

THIRD SERIES, VOLUME 33, NUMBER 7 1 APRIL 1986

Anomalous electron-spin relaxation in amorphous silicon

T. R. Askew* and H. J. Stapleton
Department of Physics and Materials Research Laboratory, University of Illinois at Urbana-Champaign, Urbana, Illinois 61801

K. L. Brower
Sandia National Laboratories, Albuquerque, New Mexico 87185
(Received 12 November 1985)

Dangling-bond electron-paramagnetic-resonance spectra and relaxation rates have been measured in the (0.3—4)-K temperature range on samples of amorphous silicon produced by sputtering, vacuum evaporation, and ion implantation of silicon, argon, neon, oxygen, and nitrogen into crystalline silicon. Intensity measurements of the dangling-bond resonance associated with silicon made amorphous by Si implantation suggest that the Curie temperature is essentially zero ($0 \leq \Theta \leq 0.03$ K) for temperatures down to 0.4 K. The relaxation rates follow unusual temperature dependencies that cannot be explained on the basis of conventional spin-phonon interactions. Instead, the relaxation rates obey a simple T^n power law in temperature where n falls within two ranges: 2.09—2.36 and 3.26—3.47. A comparison of rates at microwave frequencies of 9.3 and 16.5 GHz indicates no magnetic field dependence. A relaxation model involving spin coupling to a distribution of two-level states is consistent with the observed T^n dependence.

I. INTRODUCTION

An important series of electron paramagnetic resonance (EPR) experiments on amorphous silicon (a-Si) has been reviewed by Thomas *et al.*[1] These and other studies[2–13] employing a wide variety of preparatory and depositional techniques have shown that the $g=2.0055$ dangling-bond paramagnetic center is always present unless large amounts of hydrogen are deliberately incorporated into the sample. This has led to the general belief that unhydrogenerated a-Si is intrinsically overconstrained[14] and thus cannot be produced without dangling bonds.

While experimentalists agree that the $g=2.0055$ EPR Zeeman line in a-Si appears structureless and isotropic, major disagreements have arisen concerning the spin density, linewidth, line shape, saturation power levels, and behavior of the signal after annealing. To reconcile a variety of conflicting results, Thomas *et al.*[1] undertook an exhaustive study of evaporated a-Si and the dependence of the data on substrate temperature, deposition rate, annealing temperature, ambient contaminants during deposition, and exposure of samples to air. Using tightly controlled ultrahigh-vacuum techniques, they obtained results that were independent of deposition rate and sample thickness over a wide range and showed complete equivalence between deposition at a given substrate temperature and anneals at the same temperature of samples generated on lower temperature substrates. The spin density for samples deposited at room temperature was found to be approximately 5×10^{19} cm^{-3}. This density drops monotonically for higher annealing or substrate temperatures, dropping by a factor of 2.2 at 430 °C, where crystallites begin to form. Crystallization is complete at 630 °C where the spin density is undetectable. Thomas *et al.*[1] conclude that there must be a variety of defect states associated with the unpaired electron spins and that these anneal out at various temperatures. The distribution of defect types must be nearly continuous, otherwise structure would appear in the relationship between spin density and annealing temperature.

The line shape of all unannealed, room-temperature deposited samples is basically Lorentzian and symmetric. Upon annealing, the linewidth at 9 GHz narrows from about 8 to 5 Oe and the line shape tends slightly toward Gaussian with some asymmetry. The complications of including dipolar and possibly exchange interactions on an inhomogeneous EPR line from a randomly distributed spin system have thus far prevented conclusive statements concerning the observed linewidth.

If large exchange interactions ($-J\mathbf{S}_1\cdot\mathbf{S}_2$) are present, the strength of the EPR signal should deviate at temperatures below $|J|/k$ from a simple Curie law, $\tanh(g\mu_B H/2kT)\sim 1/T$. Thomas *et al.*[1] found a Curie law behavior between 5 and 120 K. The results of other

 ©1986 The American Physical Society

researchers have been reviewed by Khokhlov[15] and these data suggest a Curie-Weiss law $1/(T+\Theta)$ at or above ^{4}He temperatures with Θ values in the range 1.1–5 K. Thomas *et al.*[1] put an upper limit on Θ of 1 K.

The picture of *a*-Si that emerges is one of an overconstrained material containing dangling bonds that result in an isotropic, structureless, and inhomogeneously broadened EPR line at $g=2.0055$. These dangling bonds are associated with an unknown surrounding structural heterogeneity. The spatial distribution of dangling bonds in *a*-Si is also unknown. This study attempts to further elucidate the microscopic nature of *a*-Si and its paramagnetic states through the use of two additional experimental capabilities not applied by previous researchers: EPR measurements of the line shape and intensity of the amorphous resonance to temperatures as low as 0.3 K, and EPR pulse saturation and recovery measurements of the spin-lattice relaxation rate between 0.3 and 4 K.

Two aspects of the *a*-Si spin system need to be examined at temperatures below 1 K. The line shape is of interest since reduced temperatures may alter averaging and/or narrowing effects that could be obscuring underlying structure of the EPR line. An investigation of the unsaturated EPR signal strength below 1 K is needed to better limit the value of Θ in the Curie-Weiss law. Measurements in the ^{3}He temperature range should be capable of detecting Θ values as low as 0.1 K.

The second experimental technique is the direct observation of the spin system's return to thermal equilibrium after a saturating pulse. These data yield the magnitude and temperature dependence of the longitudinal relaxation time, T_1. Gourdon *et al.*[13] have published relaxation data on evaporated films of *a*-Si between 4.2 and 290 K and reported relaxation rates, $1/T_1$, that varied as T^2 below 10 K, changing to a T dependence above 30 K. They attributed this to a phonon bottleneck,[16–20] but this was shown to be in error in a preliminary report of our work on *a*-Si.[21] Stutzmann *et al.*[22] have measured the electron spin-lattice relaxation times using adiabatic passage techniques in doped and undoped *a*-Si:H and *a*-Ge:H. They claimed that the spin-lattice relaxation times for these materials is dominated by spin coupling to two level states (TLS) of the network at all temperatures up to at least 300 K. The results of our spin-lattice relaxation measurements[21] indicate that the relaxation rate in Si implanted *a*-Si varies as a simple $T^{2.37}$ power law between 0.3 and 4 K. This temperature dependence is inconsistent with conventional spin-lattice relaxation processes involving either the direct or Raman processes and suggests relaxation by a distribution of two level states.

II. EXPERIMENTAL DETAILS

A. Sample preparations

All of the samples used in this study started with 0.025-in.-thick, high-purity, *c*-Si wafers that were vacuum float-zone grown, *p* type with room-temperature resistivities above 1000 Ω cm, and had (110) faces. The wafers were cut to fit the microwave cavity of our ^{3}He probe and then etched to remove saw damage. The broad faces were polished with 30-μm diamond grit and then 50 μm was removed by etching. The samples were oriented in the cavity such that the quantity $\mathbf{H}_1 \times \mathbf{H}_0$ did not vary by more than a factor of 3 over the volume of the sample. Here $\mathbf{H}_1$ is the microwave magnetic field and $\mathbf{H}_0$ is the applied static field, parallel to [110]. Each side of the wafer was amorphized separately in successive production runs under identical conditions. The result was an amorphous region with a surface area of 3.2 cm^2 and a depth between 3600 and 13 000 Å, depending on the process. Three different processes were used to prepare samples for this study: various types of ion implantation into *c*-Si, vacuum condensation of Si vapor created by electron-beam heating and sputtering. In the last two processes the wafers discussed above function only as substrates for the amorphous films.

In this study, ion implantation was used as a tool for producing very pure *a*-Si with consistent sample characteristics and minimal H, C, and O contamination. Ion implantation converts *c*-Si to *a*-Si by producing clusters of highly disordered Si which coalesce to form a continuous random phase if the dose is high enough.[23,24] It is possible, with careful manipulation of substrate temperature and orientation, and projectile energy, mass, and fluence, to produce a thick and continuous amorphous layer with a relatively small volume of clustered and defect ridden *c*-Si. In this work the ion beam was oriented 5° off of ⟨110⟩ to avoid channeling. The samples were held at room temperature by large heat sinks.

Methods for calculating the distribution of ion energy deposition into atomic displacement have been developed by Brice[25] and Winterbon.[26] These methods are derived from the range-energy relations of Lindhard and others,[27] which are reviewed by Gibbons.[28] The calculations of Brice[29] include the contributions of recoiling target atoms, are available in tabular form,[30] and were used in this study. Because the ions produce the most atomic displacement when their energy is below 50 keV, the damage in the crystal is concentrated at a depth somewhat less than the projected range but well in from the surface. Various data indicate that the atomic displacement energy density threshold for production of *a*-Si in room temperature *c*-Si substrates is about 2×10^{24} eV/cm^3 or 2 eV/Å^3.[31–33] This threshold can be used to predict the depth of the amorphous region. As the lattice damage accumulates during implantation, an amorphous region is generated that spreads both inward and outward to the crystal surface. In order to minimize the volume of the damaged but nonamorphous region, sufficient fluence was used to bring the amorphous region out to the surface in all but one (No. 3) of the implanted samples. Since it is apparently impossible to ion damage *a*-Si, damage beyond the threshold produces no distinguishable permanent effects.

Six different types of samples were prepared by ion implantation and are described in Table I. The depths of the amorphous regions were calculated from Brice's theory.[25,29,30] As the mass of the implanted ion was decreased, higher fluences (at the same implantation energy) were required to make the sample amorphous out to the surface. Two results of this are a larger volume of dam-

TABLE I. Preparation conditions for samples made by ion implantation.

Sample no.	Implanted ion	Implantation energy (keV)	Fluence (cm^{-2})	Calculated depth of amorphous region (Å)
1	$^{40}Ar^{+}$	240	4×10^{15}	3600
2	$^{40}Ar^{2+}$	250	5×10^{15}	7200
3	$^{28}Si^{+}$	250	5×10^{15}	4500
4	$^{20}Ne^{2+}$	240	1.4×10^{16}	13 000
5	$^{16}O^{+}$	250	2.0×10^{16}	7900
6	$^{14}N^{+}$	240	2.3×10^{16}	8100

aged, but nonamorphous sample, and a less distinct transition from amorphous to crystalline regions. This trend was observed in the spectroscopic data. The preparation processes used for sample Nos. 1—3 were each repeated on several occasions and consistent sample properties were obtained. Sample Nos. 4—6 were individual preparations. Theory predicts an amorphous region from 65 to 4600 Å for sample No. 3.

Previous studies have primarily used *a*-Si made by evaporation and sputtering. Sample No. 7 was produced by evaporation from an electron-beam heated source under standard deposition conditions: base pressure, 4×10^{-6} torr; substrate temperature, 25 K; electron beam, 2.6 mA at 10 kV; deposition rate, 42 Å/s; film thickness, 7000 Å. Film adherence to the *c*-Si substrate was good and there was no visual evidence of spalling or cracking. Effects from contamination have been observed[1] (probably due to H, C, and O) in samples made by evaporation at pressures above 3×10^{-8} torr. This is one of the reasons for the use of ion implantation as the principal preparation method in this study.

Sample No. 8 was prepared by sputtering using a Varian *S*-type sputter gun operating at 980 V dc and 1.0 A. The base pressure was 1×10^{-6} torr and the Ar gas pressure during sputtering was 3.5×10^{-3} torr. One of the disadvantages of this method is that some of the sputtering gas is incorporated into the deposited film. The main motivation in producing this sample was to determine if the unusual phenomena observed in the Ar implanted samples were also present in the sputtered sample. The film thickness of the sputtered sample was 5000 Å (computed from deposition rate monitoring) and it adhered well to the *c*-Si substrate, showing no visible evidence of spalling or cracking.

B. Spectrometers

Spin-lattice relaxation rates were measured in this study at 16.5 GHz (*Ku* band) and 9.3 GHz (*X* band) using the pulse saturation and recovery technique with superheterodyne detection. Because of the use of pulsed microwave power levels, the klystrons were frequency stabilized using a Pound circuit[34] with an external reference cavity manually tuned to the sample cavity resonance. The achievable frequency stability was a few parts in 10^7 over a 15 min time span. The sample cavity Q was sufficiently high ($\sim$20 000) that changes in frequency larger than this produced an observable and undesired deviation in the detected output.

Power pulses were formed by microwave diode switches (90 dB at *Ku* band, 50 dB at *X* band) shunted by two crossguide couplers, a variable phase shifter, and a variable attenuator, thus allowing independent control of the saturating and monitoring power levels. The i.f. amplifiers were centered at 60 MHz with a 10 MHz bandwidth. The detected output from these amplifiers was dc shifted, dc amplified, digitized, and then averaged. An analog representation of the averaged signal was logarithmically amplified and displayed on an oscilloscope, allowing the relaxation rate, $1/T_1$, to be determined directly. These measured rates were later checked against computer-generated exponential fits to the digitized data. With simple modifications the *Ku* band EPR spectrometer could be converted into a reflectometer so that temperature-dependent reflection coefficients could be measured over a 20-dB range in reflected power.

The *Ku*-band spectrometer incorporated a ^3He refrigerator[35] as the upper wall of a cylindrical TE_{011} (wavemeter) mode cavity. This wall was thermally isolated from the other cavity walls by nylon spacers and a thin-walled cupronickel ^3He pumping line that produced temperatures as low as 0.3 K with a 150 l/s diffusion pump. Samples were inserted through the cavity bottom which was then sealed with an indium o-ring gasket. Under these conditions the remaining walls of the cavity were in contact with liquid ^4He at an approximate temperature of 1.2 K, allowing the EPR spectrum of samples at two temperatures to be compared within the same cavity. This feature was used to calibrate a germanium resistance thermometer below 1.2 K using two samples of a known Curie-law paramagnet (neodymium-doped lanthanum magnetism nitrate, LMN:Nd). Temperatures were measured and controlled to within a few millikelvin using this resistor, a 22 Ω heater attached to the refrigerator, ^3He exchange gas, and a feedback control system. All temperatures were corrected for magnetoresistance effects (<15 mK). Microwave power levels incident on the cavity during cw experiments were less than 50 pW. All of the equipment used is described in more detail elsewhere.[36]

C. Magnetization studies

The temperature dependence of a sample's magnetization below 1.2 K could be checked in a manner similar to the calibration of the temperature sensor. The sample under investigation and the LMN:Nd standard were placed in equivalent positions on the ^3He evaporation pot and their phase-sensitive-detected EPR signals were com-

pared at three different temperatures. Within experimental error the ratio of peak-to-peak derivative signal heights equalled the ratio of total area under the EPR absorption curves. The latter were mechanically computed from the first moments of the derivative spectra using an Amsler mechanical integrator. The observed equality indicates a temperature-independent line shape.

III. RESULTS

A. EPR spectroscopy

Table II lists the g factors, linewidths, and unpaired spin densities of all eight samples obtained using a third spectrometer[37] that operated at 20.3 GHz and 20 K. These samples, while not physically the same as those used for the *Ku* and *X* band studies, were prepared at the same time and under the same conditions and are thus equivalent. The g factors of the samples used at *Ku* band were checked and found to be consistent with the 20.3-GHz data of Table II. The linewidths of these samples were measured at 16.5 GHz and various temperatures between 0.3 and 4 K and were approximately 5% smaller than those in Table II. No temperature dependence was observed and the 5% difference is thought to be due to a frequency dependent component, since that is consistent with the observations of others.[1] The applied magnetic field was parallel to [110] of the silicon substrate.

The spin densities listed here were obtained by comparison of EPR signals with a well characterized sample, prepared by Gere, of degenerate P-doped c-Si that was crushed and embedded in polyethylene. The amorphous resonance was least-squares fitted to a Lorentzian line shape from which the area and spin density were calculated. Changes in cavity Q and filling factor were also taken into consideration.

EPR spectra from all the samples were examined near 2 and 0.38 K. In all cases the structure of the $g=2.0055\pm0.0005$ line remained the same at the two temperatures. A detailed analysis of sample No. 3 at $T=0.452$ indicated the spectrum was within a few percent of having a symmetric Lorentzian line shape except for a small interfering anisotropic line near $g=2.0101$. This resonance could be due to a Si-*P*3 center (a {110} planar four vacancy)[38,39] associated with clustering and/or damage in the c-Si region. Sample Nos. 1–4 exhibited similar spectra. The interfering line was smaller for the Ar implants and larger for the Ne implant. This is consistent with the increasing fractional volume of damaged but nonamorphous regions as the mass of the implanted species decreases.

Sample Nos. 5 and 6, produced by O^+ and N^+ implantations, respectively, exhibited complex spectra characteristic of molecular interactions between the implanted species and Si superimposed on a normal a-Si spectrum. The line near $g=2.0101$ was very large (40% of the $g=2.0055\pm0.0005$ line amplitude) indicative of a large fraction of damaged Si. Brosious[40] has concluded that for O^+ implantation the atomic displacement energy density threshold for the amorphization of Si is about 6 eV/Å^3 at room temperature. This is a factor of 3 higher than other investigators have found for Ar, Si, and Ne (Refs. 31–33) and predicts the large fraction of damaged c-Si that was observed. Amorphous Si made by N^+ implantation has not been investigated in detail; evidently a similar situation exists.

Sample No. 7 (electron-beam evaporation) exhibited a Lorentzian line shape with no evidence of interfering resonances. With its slight asymmetry taken into account (high-field derivative peak$=1.046\times$low-field peak) the lineshape was within 2% of Lorentzian. The peak-to-peak derivative linewidth at 16.5 GHz was 10 Oe.

The sputtered sample (No. 8) had a line shape that was intermediate between Gaussian and Lorentzian, with a peak-to-peak derivative width of 13.8 Oe at 16.5 GHz. The derivative peaks were 22% asymmetric. Contaminations have been shown to account for these phenomena.[1]

B. Magnetization

Several research groups have reported that the EPR spectrum in a-Si deviates slightly from a strict Curie-law behavior $[\tanh(h\nu/2kT)]$ and have reported deviations in terms of a Curie-Weiss law $(\tanh[h\nu/2k(T+\Theta)])$ in the high-temperature limit, $1/(T+\Theta)$. Pawlik *et al.*[41] reported a Θ value of 1.1 K from bulk susceptibility data on sputtered samples. Fritzsche and Hudgens[42] report $\Theta\sim5$ K from similar measurements on sputtered samples. Thomas *et al.*[1] saw no deviations in the temperature range 5–120 K on evaporated and ion-implanted samples and put an upper limit of ~1 K on the value of Θ. Khokhlov *et al.*[15] reported ferromagnetic ordering on a-Si with

TABLE II. Spectroscopic data for amorphous silicon. All measurements made at 20.3 GHz and 20 K with **H** parallel to [110].

Sample no.	Preparation	g factor (±0.0001)	Linewidth (±0.1 Oe)	Spin density (cm^{-3})
1	$^{40}Ar^+$ implanted	2.0058	6.1	4.2×10^{19}
2	$^{40}Ar^{2+}$ implanted	2.0058	6.3	2.2×10^{19}
3	$^{28}Si^+$ implanted	2.0059	6.3	1.7×10^{19}
4	$^{20}Ne^{2+}$ implanted	2.0058	6.0	1.1×10^{19}
5	$^{16}O^+$ implanted	2.0061	6.2	8.4×10^{18}
6	$^{14}N^+$ implanted	2.0058	6.0	2.4×10^{18}
7	evaporated	2.0057	10.2	1.1×10^{19}
8	sputtered	2.0058	13.8	1.1×10^{19}

transition temperatures in the (12—50)-K range.

Using the technique described in Sec. II, we report our results on samples Nos. 1 (a-Si:Ar^+) and 3 (a-Si:Si^+) in terms of the following temperature-dependent signal amplitude ratios $R(T)$:

$$R(T) \equiv \frac{I_{\mathrm{LMN:Nd}}(T)}{I_{a\text{-Si}}(T)} \frac{I_{a\text{-Si}}(1.250\ \mathrm{K})}{I_{\mathrm{LMD:Nd}}(1.250\ \mathrm{K})} . \quad (1)$$

The results for sample No. 1 are R(0.700 K) $=1.075\pm0.016$ and R(0.400 K) $=1.152\pm0.013$. These ratios were measured at 150-pW microwave power but were independent of microwave power between 50 and 500 pW. Each ratio represents roughly 100 amplitude comparisons and the distribution of results was Gaussian. These ratios are consistent with a Θ value of 0.22 ± 0.02 K. Alternatively, for an isotropic exchange interaction, $-J\mathbf{S}_1\cdot\mathbf{S}_2$, the ratios are consistent with a J/k value of -0.52 ± 0.02 K, indicative of an antiferromagnetic coupling.

By contrast, sample No. 3 exhibited only slight deviations from a strict Curie law and these were strongly dependent upon the microwave power level. Reduced microwave power reduced the deviation all the way down to the lowest operating power level of 50 pW. With this incident power, R(0.700 K) $=1.00\pm0.03$ and R(0.400 K) $=1.02\pm0.02$. Here again, each ratio represents approximately 100 comparisons, normally distributed, with $\pm1\sigma$ errors reported. The observed trend in the power-law dependence strongly implies that R(0.400 K) would converge to 1.00. However, the observed value of R(0.400 K) is consistent with $0\leq\Theta\leq0.03$ K and $-0.25\ \mathrm{K}\leq J/k\leq0$.

C. Spin-relaxation measurements

Care was taken to ensure that the observed spin-lattice relaxation rate was independent of the pulse duration, pulse power level, and monitor power level. The various samples were analyzed under the following standard conditions: 100-μs pulses, -40-dB monitor to pulse power ratio, 0.6 s delay between pulses. Approximately 1 μW of pulse power was used at 1 K. At other temperatures the pulse power was scaled linearly with T. No changes in the relaxation rates were observed for ±3 dB changes in the monitor power, ±6 dB changes in the monitor to pulse power ratio, or for different pulse durations within a (50—400)-μs range.

The microwave signal recoveries reported here were not exponential over their entire range of recovery. The rates we report were determined from the last portion of the recovery, where it appeared to be exponential within a few percent. This range of exponential behavior varied somewhat with temperature. At 0.4 K, recoveries were exponential over the final 35%, but this fraction dropped as low as 20% with increasing temperature.

Initial nonexponential recoveries are the rule rather than the exception, even in crystalline materials, although seldom this prolonged. This may be due in part to the fact that the EPR line is inhomogeneously broadened and to the limitations on pulse power and pulse duration imposed by our ^{3}He refrigerator. If the sample temperature changes during recovery, an apparently nonexponential recovery will be artificially induced even in a linear spin system.

The relaxation rates from sample No. 3 (a-Si:Si^+) at Ku and X band frequencies are shown in Fig. 1. Anomalous temperature and frequency dependencies are apparent. A one-phonon relaxation process, expected to dominate at these temperatures, should produce a relaxation rate with a coth($h\nu/2kT$) temperature dependence if the mechanism is not phonon limited; or a coth^2($h\nu/2kT$) temperature dependence in the limit of an extreme phonon bottleneck.[17–20] Both of these temperature dependences are shown in Fig. 1 and are forced to fit the datum near 4 K. In the case of a partial phonon bottleneck, the theoretical curve would fall between these two limiting curves. Furthermore, an ordinary one-phonon relaxation rate for an ion with an odd number of unpaired spins should show a ν^5 frequency dependence, i.e., the Ku band rates should be 17.6 times faster than the X band rates at the same temperature. In practice, a somewhat smaller frequency dependence is observed at these lower microwave frequencies, but never a complete frequency independence. Separate power-law fits for the 9.3- and 16.5-GHz data are $(167\pm11)T^{2.34\pm0.08}$ and $(169\pm12)T^{2.39\pm0.09}$, respectively. The combined fit is $(165\pm3)T^{2.36\pm0.02}$ and is represented by the solid line through the data in Fig. 1.

Figure 2 shows similar data for sample Nos. 4 (a-Si:Ne^{2+}), 7 (evaporated), and 8 (sputtered) together with the fit of sample No. 3 from Fig. 1. These rates were measured only at 16.5 GHz. All these samples showed simple power-law dependences: $(118\pm10)T^{2.34\pm0.05}$ for No. 8, $(466\pm19)T^{3.27\pm0.08}$ for No. 4, and $(740\pm43)T^{3.47\pm0.09}$ for No. 7. The frequency dependence

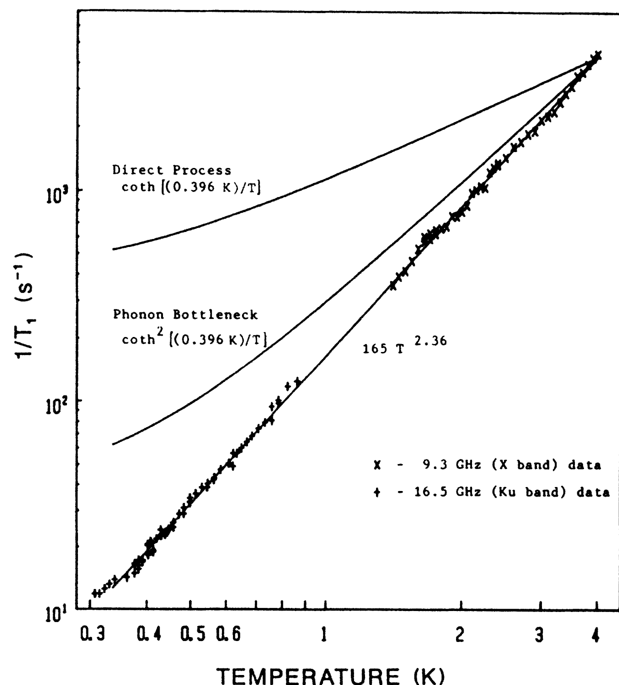

FIG. 1. Electron-spin-lattice relaxation rates for amorphous silicon made by $^{28}Si^+$ ion implantation (sample No. 3).

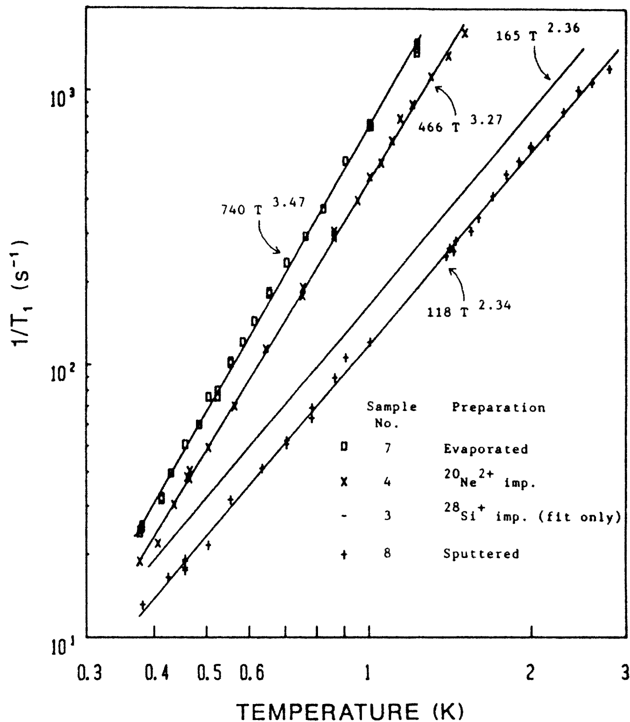

FIG. 2. Electron-spin-lattice relaxation rates for amorphous silicon made by various preparations (frequency = 16.5 GHz).

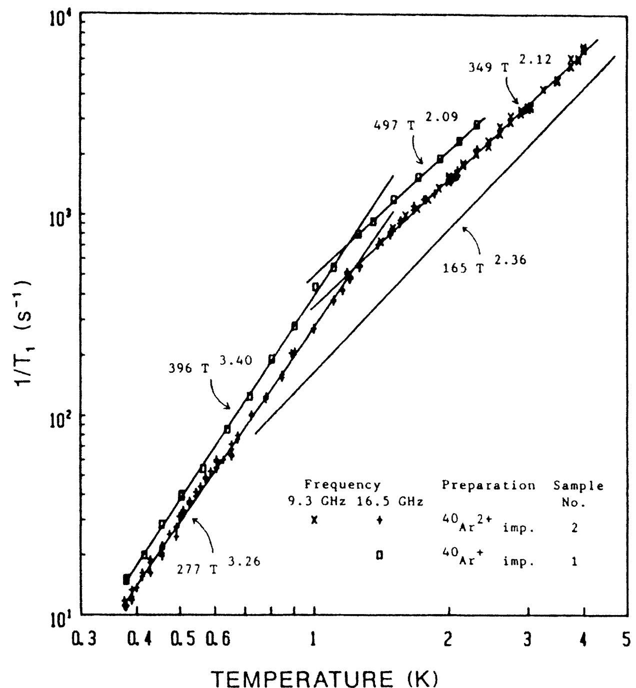

FIG. 3. Electron-spin-lattice relaxation rates for amorphous silicon made by $^{40}Ar^{+}$ and $^{40}Ar^{2+}$ ion implantation (sample Nos. 1 and 2, respectively). These data cannot be fitted to Eq. (5) of the text using a single value of E.

of the spin-lattice relaxation rate of sample No. 8 was checked at 1.5 K and the rates at 9.3 and 16.5 GHz differed by less than 1%.

Experimental results for two Ar-implanted samples (Nos. 1 and 2) are shown in Fig. 3 along with the best fit for sample No. 3. In contrast to the other samples, these data display two different power-law dependences with a sharp transition between the two near 1.2 K. Usually the transition from one dominant relaxation process to another takes place over a discernible temperature range. The data of sample No. 1 are best fitted below 1.19 ± 0.08 K by $(396\pm24)T^{3.40\pm0.10}$ and by $(497\pm23)T^{2.09\pm0.08}$ above that temperature. The best fit of the data from sample No. 2 is $(277\pm14)T^{3.26\pm0.08}$ below 1.23 ± 0.06 and $(349\pm14)T^{2.12\pm0.04}$ above that temperature. The latter fit includes both *Ku*- and *X*-band relaxation data and no significant frequency dependence is observed.

It is worth noting that while the Ar-implanted samples both showed this transition at 1.2 K between two different power laws, the sputtered sample (No. 8) showed no similar transition temperature. It is estimated the sputtered sample contained 1—2 at. % Ar, while the Ar-implanted samples contained 0.2 at. % in their amorphous regions.

Spin recovery profiles for sample Nos. 5 and 6 were found to be badly nonexponential at temperatures above 0.45 K. Even when the recoveries approached exponential near 0.3 K, the rates were strongly dependent on what portion of the EPR spectrum was probed. Since these samples also had interfering spectra, no further relaxation data were taken.

For the six samples studied, the temperature exponents fell into two narrow ranges: 2.09—2.36 and 3.26—3.47. In addition, there appears to be an interesting correlation between the spin-relaxation-rate prefactor and the deviation of the exponent from 2. The relaxation rates from sample Nos. 3, 4, 7, and 8 can all be fitted to within 18% by

$$1/T_1 = 419\lambda T^{2+\lambda} . \tag{2}$$

IV. POSSIBLE RELAXATION MECHANISM

We are faced with finding a mechanism that predicts a relaxation rate varying below 10 K as a simple power law in temperature with an exponent slightly greater than 2.00, but reducing to a linear temperature dependence above 30 K. This linear T dependence in the classical limit of these higher temperatures eliminates the involvement of more than one phonon. A simple one-phonon relaxation rate must follow a $\coth(h\nu/2kT)$ dependence, while a phonon-limited direct rate varies as $\coth^2(h\nu/2kT)$. As shown by Fig. 1, neither of these dependences even approximates the observed temperature variation.

A possible mechanism involving localized two level states (TLS) and a single phonon was simultaneously suggested by Stutzmann *et al.*[43] and Askew *et al.*[44] Two level states are tightly coupled to the phonon system. Therefore if a spin is coupled to a nearby TLS, it may relax through it. Two different modes of spin relaxation via TLS have been independently proposed[45,46] but they have been shown to be closely related.[47] It is the unpublished mechanism proposed by Lyo and Orbach,[46] which was

later modified to explain the T^2 temperature dependence of the homogeneous optical linewidths in amorphous materials,[48] that appears to explain these relaxation data in a-Si.

Phillips[49] has reviewed the use of the TLS model for interpreting experimental data from amorphous materials. The original form of this model was proposed independently by Anderson *et al.*[50] and Phillips.[51] They suggested that atoms or configurations of atoms tunneling within a double-well potential might be responsible for the system of TLS found useful in describing the low-temperature data of amorphous materials. Thermal properties of a-Si:H (Ref. 52) and of hydrogen-free a-Ge (Ref. 53), for example, have been explained on the basis of two level states.

We consider the following Hamiltonian operators to describe the TLS-phonon interaction ($\mathscr{H}_{T\text{-ph}}$) and the TLS-spin interaction ($\mathscr{H}_{T\text{-}S}$):

$$\mathscr{H}_{T\text{-ph}} = \frac{1}{2} \begin{bmatrix} D & M \\ M & -D \end{bmatrix} e \tag{3}$$

and

$$\mathscr{H}_{T\text{-}S} = B(S_+ + S_-) \begin{bmatrix} C & N \\ N & -C \end{bmatrix} , \tag{4}$$

where e is a scalar approximation to the acoustic strain, S_+ and S_- are spin raising and lowering operators, and B, C, D, M, and N are parameters. The TLS have energies of $\pm E/2$, assumed much larger than the spin-state energies of $\pm\delta/2$. The reader is referred to Eqs. (7)–(10) and Fig. 6 of Ref. 47 for a detailed understanding of the computation that follows. The major changes from the referenced calculation lie in the altered forms of $\mathscr{H}_{T\text{-ph}}$ and $\mathscr{H}_{T\text{-}S}$.

If all TLS had an energy splitting E, the relaxation rate of the spins would be

$$\frac{1}{T_1(E)} = \frac{12B^2}{\pi h^4 \rho v^5} \left[\frac{CM}{\delta} - \frac{ND}{E} \right]^2 \frac{E^3}{\sinh(E/kT)} . \tag{5}$$

Here ρ is the mass density and v is the velocity of sound.

If $CM/\delta \gg ND/E$ in Eq. (5), the mechanism proposed by Kurtz and Stapleton[45,47] results. If the inequality is reversed, the mechanism proposed by Lyo and Orbach[46,48] is produced. The observed spin-relaxation rate is now approximated by averaging $1/T_1(E)$ over the energy distribution, $P(E)$, of the TLS:

$$\langle 1/T_1 \rangle \sim \int_{E_{\min}}^{E_{\max}} dE\, P(E)/T_1(E) \Big/ \int_{E_{\min}}^{E_{\max}} dE\, P(E) . \tag{6}$$

The TLS model assumes that $P(E)$ is weakly dependent upon E and is represented by an E^λ power law within some range $E_{\min} \le E \le E_{\max}$, with λ small and positive. Typically, glasses are characterized by $E_{\min}/k \sim 10^{-3}$ K and $E_{\max}/k \sim 10$ K. The mechanism proposed by Lyo and Orbach then yields $\langle 1/T_1 \rangle$ rates varying as $T^{2+\lambda}$ in the simplest case ($E_{\min} < kT, E_{\max} \gg kT$), whereas the other term in Eq. (5) leads to $T^{4+\lambda}$ under similar conditions. Considering only the former, Eq. (6) becomes

$$\langle 1/T_1 \rangle \propto B^2 T^{2+\lambda} \int_{x_{\min}}^{x_{\max}} \frac{x^{1+\lambda}}{\sinh x} dx , \tag{7}$$

with $x = E/kT$. At high temperatures ($kT > E_{\max}$), $\langle 1/T_1 \rangle$ becomes linear in T in agreement with the experimental data of Gourdon *et al.*[13] The frequency independence of our results requires that B be independent of the applied magnetic field. Data from Ref. 22 imply B is proportional to the spin-orbit coupling constant. Deville *et al.*[54] have observed electron-spin-lattice relaxation rates of V^{4+} in amorphous V_2O_5 and found behavior described by Eq. (7) with $\lambda \approx 0$.

Although this model correctly predicts the observed $H^0 T^n$ dependence of the relaxation rates in a-Si, modifications are required for its use at the low temperatures employed in this study. In previous calculations of this type it has always been assumed that $E_{\min} \gg \delta$ and $E_{\min} < kT$, but in these experiments $\delta = kT$ at 0.792 K.

The effects of two revisions must be considered. The first is that δ/E is no longer negligible compared to unity and the thermal factors that ordinarily sum to $(\sinh E/kT)^{-1}$ will no longer do so. The second involves a reexamination of the phonon-induced transition (see Fig. 6 of Ref. 47) between a combined spin TLS of energy $(E-\delta)/2$ and one of energy $(-E+\delta)/2$ when E is less than or equal to δ. These corrections have been considered.[36] The predicted temperature dependence is

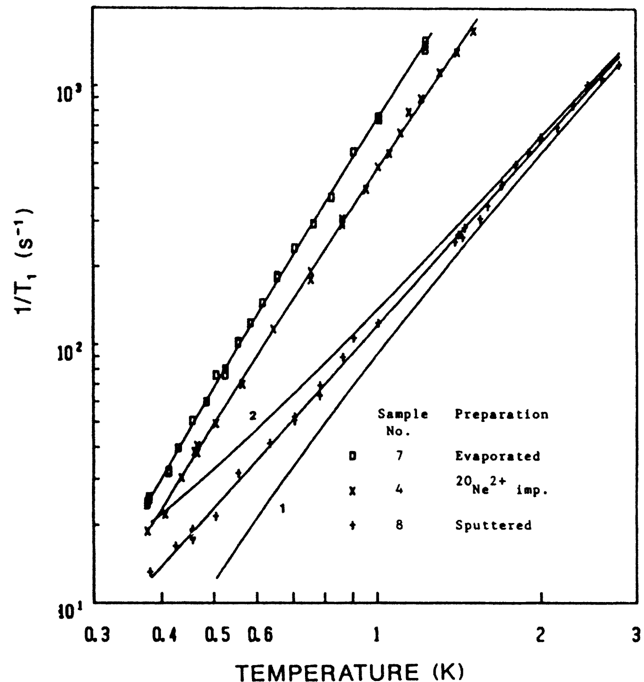

FIG. 4. Electron-spin-lattice relaxation rates for amorphous silicon made by various preparations [frequency = 16.5 GHz, data fits are from Eq. (8)]. Curves 1 and 2 are discussed in the text.

TABLE III. Results of a modified analysis of a-Si relaxation data. Shown are prefactors for Eq. (8) and the best fitting values of λ and $E_{\min}/k$. Shown also are the corresponding simple power-law fits.

Sample no.	Preparation	Power-law-fit	Modified theory Prefactor	λ	$E_{\min}/k$ (K)
3	$^{28}Si^{+}$ implanted	$(165\pm3)T^{2.36\pm0.02}$	16.8	0.32 ± 0.08	0.59 ± 0.10
4	$^{20}Ne^{2+}$ implanted	$(466\pm19)T^{3.27\pm0.08}$	27.0	1.10 ± 0.13	1.10 ± 0.12
7	evaporated	$(740\pm43)T^{3.47\pm0.09}$	38.1	1.22 ± 0.14	1.23 ± 0.14
8	sputtered	$(118\pm10)T^{2.34\pm0.05}$	12.2	0.29 ± 0.08	0.58 ± 0.11

$$\langle 1/T_1 \rangle \propto T^{2+\lambda} \int_{x_{\min}}^{x_{\max}} dx \frac{x^{\lambda}}{\sinh x} \left[2x + \frac{(x+y)(e^{x}-e^{y})}{e^{x+y}-1} + \frac{(x-y)(e^{x}-e^{-y})}{e^{x-y}-1} \right], \tag{8}$$

where $x=E/kT$ and $y=\delta/kT$. With $x_{\max}$ effectively at infinity, certain combinations of λ and $E_{\min}$ result in rates which very closely follow the T^{n} power laws that describe the data so well. For example, the best fit of Eq. (8) to the data from sample No. 8 (sputtered) resulted in the values $E_{\min}/k=0.58$ and $\lambda=0.29$. This function is shown in Fig. 4 and deviates from the simple power-law fit, $T^{2.34}$, by no more than 1% between 0.3 and 3 K. The function specified by Eq. (8) is sensitive to the value of $E_{\min}/kT$, particularly at temperatures below 1 K. Curves 1 and 2 of Fig. 4 show the result of changing $E_{\min}/k$ from 0.58 K to 1.2 and 0.0 K, respectively.

Table III lists the values of λ and $E_{\min}/k$ that best fit the data of sample Nos. 3, 4, 7, and 8. The resulting fits to the data are not significantly better than the simple power-law fits predicted by Eq. (7). It is puzzling that the relaxation data follow strict power laws in this temperature regime. Equation (8) predicts such behavior only as a special case involving anomalously large values of $E_{\min}$. Also not explained is the apparent correlation between the prefactors and the amount by which the temperature exponent exceeds 2.0.

A complete TLS model of spin relaxation in a-Si would specify the nature of the TLS-spin interaction. We are still unable to do so after additional electron-nuclear double resonance and microwave frequency dielectric susceptibility measurements, performed on a-Si:Si for this purpose, failed to yield pertinent data.

V. CONCLUSIONS

Conventional spin-phonon interactions cannot account for the measured $H^{0}T^{n}$ temperature dependence of the electron-spin-relaxation rates in various samples of a-Si over a temperature range of 0.3—4.0 K. The n values for six samples fell into two ranges: 2.09—2.36 and 3.26—3.47. Distinct differences in the spin-lattice relaxation rates, which are reasonably reproducible, are observed among samples of amorphous silicon prepared by different methods. However, the specific features in the atomic structure of amorphous silicon and/or the role of impurities responsible for these effects remain as of yet unknown. A phenomenological quantum-mechanical model involving spin coupling to a distribution of two level states has been presented that is capable of representing the temperature dependence of the spin-lattice relaxation rate. The model does not predict the observed correlation between the rate prefactor and $n-2$, nor does it explain the sharp transition in the temperature exponent observed for two Ar-implanted samples at 1.2 K. No new spectroscopic features appeared in the EPR spectra for temperatures down to 0.3 K. Deviations from a Curie-law paramagnetism were found for Ar-implanted a-Si, but no significant deviation was found for Si-implanted samples of a-Si. Thus, in the case of pure amorphous silicon, the lack of any significant spin-spin interactions is consistent with a dilute distribution of unpaired spins.

ACKNOWLEDGMENT

This work was supported by the U.S. Department of Energy (Division of Materials Sciences), under Contracts No. DE-AC02-76ER01198 and No. DE-AC04-76DP00789.

*Present address: Engineering Physics Laboratory (E-357205), E.I. du Pont de Nemours and Company, Wilmington, DE 19898.

[1]P. A. Thomas, M. H. Brodsky, D. Kaplan, and D. Lepine, Phys. Rev. B **18**, 3059 (1978).

[2]J. Stuke, *Proceedings of the Seventh International Conference on Amorphous Semiconductors, Edinburgh, 1977*, edited by W. E. Spear (University of Edinburgh Press, Edinburgh, 1977), p. 406.

[3]U. Voget-Grote, J. Stuke, and H. Wagner, *Conference on the Structure and Excitations of Amorphous Solids, Williamsburg, Virginia, 1976*, edited by G. Lucovsky (AIP, New York, 1976), p. 91.

[4]U. Voget-Grote, W. Kummerle, R. Fischer, and J. Stuke, Philos. Mag. **41**, 127 (1980).

[5]B. Movaghar and L. Schweitzer, Phys. Status Solidi B **80**, 491 (1977).

[6]B. Movaghar and L. Schweitzer, Philos. Mag. B **37**, 683 (1978).

[7]R. Bachus, B. Movaghar, L. Schweitzer, and U. Voget-Grote, Philos. Mag. B **39**, 27 (1979).

[8]S. Hasegawa and S. Yazaki, Solid State Commun. **23**, 41 (1977).

[9]S. Hasegawa, T. Kasajima, and T. Shimizu, Solid State Commun. **29**, 13 (1979).

[10]T. Shimizu, M. Kumeda, I. Watanabe, and K. Kamond, Jpn. J. Appl. Phys. **18**, 1923 (1979).

[11]N. Ishii, M. Kumeda, and T. Shimizu, Jpn. J. Appl. Phys. **20**, L673 (1981).

[12]M. Suzuki, M. Suzuki, M. Kanada, and Y. Kakimoto, Jpn. J. Appl. Phys. **21**, L89 (1982).

[13]J. Gourdon, P. Fretier, and J. Pescia, J. Phys. (Paris) Lett. **42**, L21 (1981).

[14]H. Fritzsche, in *What are Non-Crystalline Semiconductors,* Vol. 25 of *Fundamental Physics of Amorphous Semiconductors,* edited by F. Yonezawa (Springer-Verlag, New York, 1981), p. 1.

[15]A. F. Khokhlov, A. I. Mashin, and A. M. Satanin, Phys. Status Solidi B **105**, 129 (1981). Note: This reference uses nonstandard terminology for Curie and Néel temperatures.

[16]J. H. Van Vleck, Phys. Rev. **59**, 724 (1941); 730 (1941).

[17]B. W. Faughnam and M. W. P. Strandberg, Phys. Chem. Solids **19**, 155 (1961).

[18]P. L. Scott and C. D. Jeffries, Phys. Rev. **127**, 32 (1962).

[19]R. C. Mikkelson and H. J. Stapleton, Phys. Rev. **140**, A1968 (1965).

[20]P. J. Muench, T. R. Askew, J. T. Colvin, and H. J. Stapleton, J. Chem. Phys. **81**, 63 (1984).

[21]T. R. Askew, P. J. Muench, H. J. Stapleton, and K. L. Brower, Solid State Commun. **49**, 667 (1984).

[22]M. Stutzmann and D. K. Biegelsen, Phys. Rev. B **28**, 6256 (1983).

[23]D. J. Mazey, R. S. Nelson, and R. S. Barnes, Philos. Mag. **17**, 1145 (1968).

[24]R. S. Nelson and D. J. Mazey, Can. J. Phys. **46**, 689 (1968).

[25]D. K. Brice, Radiat. Eff. **6**, 77 (1970).

[26]K. B. Winterbon, Radiat. Eff. **13**, 215 (1972).

[27]J. Lindhard and M. Schraff, Phys. Rev. **124**, 128 (1961).

[28]J. F. Gibbons, Proc. IEEE **56**, 295 (1968).

[29]D. K. Brice, J. Appl. Phys. **46**, 3385 (1975).

[30]D. K. Brice, *Ion Implantation Range and Energy Deposition Distributions* (Plenum, New York, 1975), Vol. 1.

[31]H. J. Stein, F. L. Vook, D. K. Brice, J. A. Borders, and S. T. Picraux, in *Ion Implantation,* edited by F. H. Eisen and L. T. Chadderton (Gordon and Breach, London, 1971), p. 17.

[32]B. L. Crowder and R. S. Title, in *Ion Implantation,* Ref. 31, p. 87.

[33]F. L. Vook, in *International Conference on Radiation Damage and Defects in Semiconductors, Reading, England, 1972* (IOP, London, 1973), p. 60.

[34]C. P. Poole, *Electron Spin Resonance* (Interscience, New York, 1967), p. 199.

[35]This refrigerator is a modified and rebuilt version of one described in detail by T. L. Bohan and H. J. Stapleton, Rev. Sci. Instrum. **39**, 1707 (1968).

[36]T. R. Askew, Ph.D. thesis, University of Illinois at Urbana-Champaign, 1984.

[37]K. L. Brower, Rev. Sci. Instrum. **48**, 135 (1977).

[38]K. L. Brower, Radiat. Eff. **8**, 213 (1971).

[39]K. L. Brower, in *Ion Implantation in Semiconductors 1976,* edited by F. Chernow *et al.* (Plenum, New York, 1977), p. 427; K. L. Brower, F. L. Vook, and J. A. Borders, Appl. Phys. Lett. **15**, 208 (1969).

[40]P. R. Brosious, in *Ion Implantation in Semiconductors 1976,* Ref. 39, p. 417.

[41]J. R. Pawlik, G. A. N. Connel, and D. Prober, in *Proceedings of the Sixth International Conference on Amorphous Semiconductors, Leningrad, 1975,* edited by W. E. Spear (Ioffe Institute, Leningrad, 1976), p. 304.

[42]H. Fritzsche and S. J. Hudgens, in *Proceedings of the Sixth International Conference on Amorphous Semiconductors,* Ref. 41, p. 6, see also S. J. Hudgens, Phys. Rev. B **14**, 1547 (1976).

[43]M. Stutzmann, D. K. Biegelsen, and J. Stuke, Bull. Am. Phys. Soc. **28**, 532 (1983). This abstract actually discusses a Raman relaxation mechanism that was corrected in the oral presentation.

[44]T. R. Askew, P. J. Muench, and H. J. Stapleton, Bull. Am. Phys. Soc. **28**, 533 (1983). This abstract does not contain a discussion of the relaxation mechanism that was orally presented.

[45]S. R. Kurtz and H. J. Stapleton, Phys. Rev. Lett. **42**, 1773 (1979).

[46]S. K. Lyo and R. Orbach (private communication).

[47]S. R. Kurtz and H. J. Stapleton, Phys. Rev. B **22**, 2195 (1980).

[48]S. K. Lyo and R. Orbach, Phys. Rev. B **22**, 4223 (1980).

[49]W. A. Phillips, *Amorphous Solids: Low Temperature Properties,* edited by W. A. Phillips (Springer-Verlag, New York, 1981).

[50]P. W. Anderson, B. I. Halperin, and C. M. Varma, Philos. Mag. **25**, 1 (1971).

[51]W. A. Phillips, J. Low Temp. Phys. **7**, 351 (1972).

[52]J. E. Graebner, B. Golding, L. C. Allen, J. C. Knights, and D. K. Biegelsen, Phys. Rev. B **29**, 3744 (1984).

[53]J. E. Graebner and L. C. Allen, Phys. Rev. Lett. **51**, 1566 (1983).

[54]A. Deville, B. Gaillard, and C. Blanchard, J. Phys. (Paris) **44**, 77 (1983).